Predictability of the Indian Ocean sea surface temperature anomalies in the GFDL coupled model

Qian Song,[1] Gabriel A. Vecchi,[2] and Anthony J. Rosati[2]

Received 7 September 2007; revised 9 November 2007; accepted 27 November 2007; published 16 January 2008.

[1] We explore the predictability of the sea surface temperature anomalies associated with the Indian Ocean Dipole/Zonal Mode (IODZM) at a three-season lead, within the Geophysical Fluid Dynamics Laboratory (GFDL) coupled general circulation model (CGCM). In both control simulations and retrospective forecasts of the 1990's in the CGCM, we find that the occurrence of some IODZM events is preconditioned by oceanic conditions and potentially predictable three seasons in advance, while other IODZM events appear to be triggered by weather noise and have low predictability. The results highlight the necessity for future studies to distinguish periods when the IODZM is more or less predictable and search for its precursory pattern in the ocean. **Citation:** Song, Q., G. A. Vecchi, and A. J. Rosati (2008), Predictability of the Indian Ocean sea surface temperature anomalies in the GFDL coupled model, *Geophys. Res. Lett.*, *35*, L02701, doi:10.1029/2007GL031966.

1. Introduction

[2] *Saji et al.* [1999] and *Webster et al.* [1999] described the extreme sea surface cooling events that occur during boreal autumn in the eastern tropical Indian Ocean off the coast of Java/Sumatra that arises from atmosphere-ocean coupled feedbacks. The anomalous cooling is often accompanied by anomalous warming in the western tropical Indian Ocean, and the resultant east-west SSTA gradient has prompted the definition of the anomalous events as Indian Ocean Dipole/Zonal Mode (IODZM) [e.g., *Saji et al.*, 1999; *Webster et al.*, 1999; *Murtugudde et al.*, 2000]. Since then, the IODZM has become focus of much research, and much has been learned about its dynamics, its relationship to the El Niño/Southern Oscillation (ENSO) and its regional/global impacts [see *Yamagata et al.*, 2004; *Annamalai and Murtugudde*, 2004, and references therein]. The evolution of IODZM anomalies is distinctively locked to seasons: appearance in Boreal Spring, growth through Boreal Summer, peak in Boreal Fall and decay in Boreal Winter. Atmosphere-thermocline coupled feedbacks, especially in the eastern Indian Ocean off Java/Sumatra, are critical for the growth of anomalies related to IODZM. Like other large-scale climate variations, IODZM is capable of bringing climate variability in various parts of the globe through teleconnection. For instance, it has been suggested that IODZM has significant impacts on the Asian monsoon, the east African rainfall, the Indonesian-Australian rainfall, and potentially the El Niño - Southern Oscillation (ENSO). Such IODZM teleconnections and their societal and economical consequences spur the desire to predict the occurrence of IODZM events.

[3] Recently, *Wajsowicz* [2004, 2005a, 2005b] made pioneering efforts in studying the predictability of the Indian Ocean SST anomalies (SSTAs) associated with IODZM, by analyzing the ensemble forecasts from the NASA Seasonal-to-Interannual Prediction Project coupled model forecast system. These studies showed that, for certain seasons, the forecast of SSTA is skillful at 3-month lead in the east pole of IODZM (ETIO; 90°E–110°E, 10°S-EQ) and at 6-month lead in the west pole of IODZM (WTIO; 50°E–70°E, 10°S–10°N), and that the potential predictability of boreal fall SSTAs at the two poles at lead time 2–3 seasons is limited. Subsequently, *Luo et al.* [2007] evaluated the IODZM predictability and its seasonal dependence in the SINTEX-F coupled general circulation model. They find a similar effective forecast range in their model, but also indicate that some IODZM event can be predicted successfully in a 9–12 month lead time.

[4] *Annamalai et al.* [2003] and *Song et al.* [2007] suggest that there are precursory patterns in boreal spring in the western equatorial Pacific for the development of IODZM. This suggests the possibility of forecasting of IODZM related anomalies in boreal fall from boreal spring or even earlier. In this study we explore such possibility in a state-of-the-art global coupled ocean-atmosphere-land-ice model recently developed at the Geophysical Fluid Dynamics Laboratory (GFDL) of U. S. National Oceanic and Atmospheric Administration (NOAA). We focus on the potential predictability of IODZM in the free-running GFDL model through a series of ''perfect model/perfect observation'' predictability experiments (see below).

2. Model and Experiments

2.1. Model Description

[5] The model used in this study is the GFDL CM2.1 version global coupled atmosphere-ocean-land-ice model. The CM2.1 coupled model is one of the models that have been employed to conduct climate sensitivity experiments for the Fourth Report of the Intergovernmental Panel for Climate Change (IPCC-AR4), and its representation of coupled processes in the Indo-Pacific is among the best of the IPCC-AR4 models [e.g., *van Oldenborgh et al.*, 2005; *Saji et al.*, 2006]. The ocean component of the coupled model is based on the GFDL Modular Ocean Model version 4 [*Griffies et al.*, 2003]. The model ocean has

[1]Program in Atmospheric and Oceanic Sciences, Princeton University, Princeton, New Jersey, USA.
[2]NOAA Geophysical Fluid Dynamics Laboratory, Princeton, New Jersey, USA.

0094-8276/08/2007GL031966$05.00

50 vertical layers with 10 m resolution in the upper 220 m. The ocean horizontal resolution is 1° × 1°, and near the Equator the meridional resolution gradually reduces to 1/3°. Model insolation varies diurnally, and shortwave penetration depth varies spatially and climatologically. The model has an explicit free surface, with explicit freshwater fluxes between ocean, land, cryosphere and atmosphere. The atmosphere component [*GFDL Global Atmospheric Model Development Team* (*GAMDT*), 2004] has a finite volume dynamic core with 24 vertical layers and 2.5° (in longitude) × 2° (in latitude) horizontal spacing. Various components of the coupled model (atmosphere, ocean, land and sea-ice) exchange fluxes every two hours, and fluxes are conserved within machine precision. More details of the model configuration and its simulations of various aspects of the climate system are given by *Delworth et al.* [2006] (coupled model), *Gnanadesikan et al.* [2006] (ocean model), *GAMDT* [2004] (atmosphere model), *Stouffer et al.* [2006] (climate sensitivity), *Wittenberg et al.* [2006] (Pacific Ocean), and *Song et al.* [2007] (Indian Ocean). This climate model has certain biases in its Indian Ocean of relevance to studies of the IODZM: a bias towards a deeper than observed Indian Ocean thermocline, and the model is more skewed towards positive IODZM events and has a higher standard deviation of SSTA than observations [*Song et al.*, 2007]. However, the model IODZM generally compares well with observations, and its composite behavior is quite similar to that observed [*Song et al.*, 2007].

2.2. Ensemble Experiments

[6] To study the potential predictability of IODZM in the GFDL coupled model, we run a Control simulation with the model to generate a pseudo-reality, and subsequently predict the IODZM events realized in the pseudo-reality. The Control simulation is a 300-year numerical integration with the GFDL CM2.1 model under the forcing of 1990 values of tracer gases, insolation, aerosols, and land cover. We only look at the last 250 years of simulation so as to eliminate initial adjustment processes. *Song et al.* [2007] found that this Control simulation reproduces fundamental characteristics of the climatology of the Indian Ocean climate, such as the west-to-east downward tilted equatorial thermocline. It also successfully simulates key features of the interannual SST variability of the Indian Ocean, the occurrence of IODZM events, and the statistical correlation between IODZM and ENSO.

[7] In this study we focus on the prediction of positive IODZM events (SST cooling in the eastern tropical Indian Ocean; referred to as "IODZM events" for simplicity), setting aside the prediction of normal and negative IODZM years for a future study. We first randomly select 10 IODZM years from the Control simulation, and 9-member ensemble prediction of each of these ten IODZM years from January 1st to December 31st is performed. With the assumption that predictability of large-scale air-sea coupled climate phenomena such as IODZM at the lead of a few seasons comes from slow-varying oceanic conditions whereas atmospheric conditions provide noise, we perturb atmospheric initial conditions among ensemble members while keeping oceanic initial conditions the same. The different initial atmospheric conditions are the daily atmospheric initial states from the Control simulation since January 2nd to 10th of the corresponding IODZM year. Additional experiments show that modifying the perturbation scheme (such as using January 1st atmospheric states of various years, or increasing the spacing of daily atmospheric states) does not significantly affect our results. Information about the predictability of those IODZM events can be obtained from the spread of ensemble members, which is discussed below.

3. Potential Predictability

3.1. IOD Predictability

[8] We adopt the IODZM index defined by *Saji et al.* [1999], which is the SSTA of its west pole (90°E–110°E, 10°S-EQ) minus the SSTA of the east pole (50°E–70°E, 10°S–10°N). We identify an IODZM event according to the criterion that the IODZM index exceeds $+1\sigma$ (the standard deviation σ of the IODZM index is computed from the 300-year control simulation) for 5 consecutive months. Note that the same criterion is used to identify IODZM events from the control simulation.

[9] The IODZM indices of the ensemble simulations of the 10 IODZM events are shown in Figure 1. It is conspicuous in Figure 1 that the IODZM events fall into two categories based on the behavior of the IODZM in the ensembles: predictable (Figure 1, bottom) and random (Figure 1, top). The ensembles of the predictable category produce substantially more IODZM events than those of the random category. We also note that the IODZM indices of nearly all ensemble members of predictable IODZM events are positive during boreal fall (which is the peak season of IODZM anomalies), whereas only a portion of the ensemble members of random IODZM events show positive IODZM index. Furthermore, the spread of ensemble members during fall (measured by the standard deviation of the IODZM index) is much smaller in the predictable IODZM events than in the random ones; the ensemble means of predictable IODZMs are fairly close to the truth while those of random IODZMs do not predict IODZM events at all. Therefore, the potential predictability of the IODZM events in the predictable category is much higher than that of the random category.

[10] We now perform a statistical hypothesis test to quantitatively distinguish the two categories of IODZM events. In the 300-year control simulation there are 45 IODZM events (identified by the same criterion of IODZM index greater than $+1\sigma$ for 5 consecutive months). If we consider the occurrence of IODZM as a random phenomenon, the statistical estimate of the probability of the IODZM occurrence is 45/300 = 0.15. We can now form a statistical hypothesis test to see whether the reproduced IODZM events in each ensemble are distinct from the background distribution. The null (H_0) and alternative (H_1) hypotheses are:

[11] H_0: the probability of IODZM occurrence (P) in an ensemble is not distinguishable from the background probability, i.e. $P <= 0.15$.

[12] H_1: the probability of IODZM occurrence (P) in an ensemble is higher than the background probability, i.e. $P > 0.15$.

[13] We use a Binomial test, for which the 95% significant level with a 9-member ensemble is $n \geq 4$ (n is the

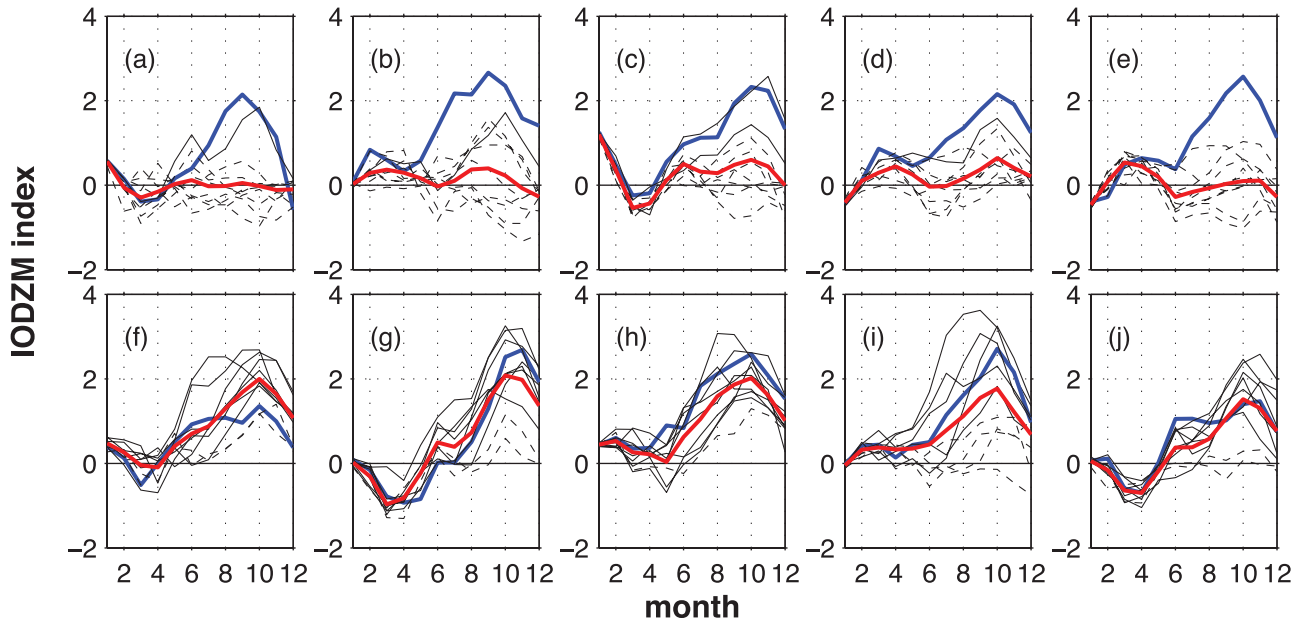

Figure 1. The IODZM index of the ten ensemble experiments. The blue curves are the pseudo-reality from the Control simulation. The solid black curves are the ensemble members that are IODZM events, and the dashed black curves are the members that are not IODZM events. The red curves are ensemble mean. The GFDL-CM2.1 standard deviation for the IODZM-I is 0.72°C.

number of IODZM events in each ensemble). Therefore, the null hypothesis is rejected for the ensembles in Figure 1 (bottom), but cannot be rejected for the ensembles in Figure 1 (top). We further hypothesize that during predictable IODZM years the climate system is preconditioned for the development of IODZM, while the random IODZM events are triggered by weather noise. That hypothesis is discussed in detail in section 4.

[14] We note that the half-half partition of the 10 selected IODZM events between the predictable and random categories may be an accident, rather than a norm (the 95% limits on the population probability based on a sample five positives in ten trials is 0.22 to 0.78). Ensemble prediction experiments with more IODZM events are needed to better quantify such statistics.

3.2. Relationship With ENSO

[15] The relationship between the IODZM and ENSO has been much debated [e.g., *Baquero-Bernal et al.*, 2002; *Huang and Kinter*, 2002; *Krishnamurthy and Kirtman*, 2003; *Fischer et al.*, 2004]. It has been argued that because IODZM events have occurred without El Niño (e.g., 1961, 1994) and there are only weak correlations between the IODZM index and ENSO indices, the IODZM is a mode independent of ENSO [e.g., *Webster et al.*, 1999; *Saji et al.*, 1999; *Iizuka et al.*, 2000; *Rao et al.*, 2002]. However, it has been noted that, because seasonally stratified correlations between the IODZM index and ENSO indices become substantially higher, aspects of the IODZM may be considered as forced by ENSO [e.g., *Baquero-Bernal et al.*, 2002; *Gualdi et al.*, 2003].

[16] The ensemble prediction experiments provide an opportunity to examine the relationship between the predictability of IODZM and ENSO. The NIÑO3 indices of the ensembles are shown in Figure S1 of the auxiliary material[1]. In "reality" (blue curves in Figure S1), all predictable IODZM events occur along with El Niño conditions, whereas the random IODZM events can occur with either El Niño or La Niña conditions. Furthermore, we notice that there is only one random IODZM event co-occurring with El Niño (see Figure S1d). In our experiments five of the six IODZM events that co-occurred with El Niño are predictable, suggesting that the chance that an IODZM event is predictable is high if it occurs along with El Niño.

4. Oceanic Initial Conditions

[17] We hypothesized in section 3 that the occurrence of predictable IODZM events had some common characteristic in their initial conditions. It is conceivable that the identification of such a signature would have substantial practical value. As we kept the oceanic initial conditions the same in each ensemble, such deterministic signature, if any, would exist in the ocean, presumably in the ocean temperature field. We compare the composite initial condition of upper ocean heat content between the two categories (Figure 2). The ocean heat content of predictable IODZM differs from that of random IODZM by having noticeable anomalous warming in the western/central equatorial Pacific Ocean and anomalous cooling in the eastern Indian Ocean. To verify that these temperature anomalies are indeed responsible for the predictability of IODZM, we conduct two 9-member ensemble experiments where the composite temperature fields of the predictable and random IODZM are separately used to initialize the model. The initial atmosphere, land, ice

[1]Auxiliary materials are available in the HTML. doi:10.1029/2007GL031966.

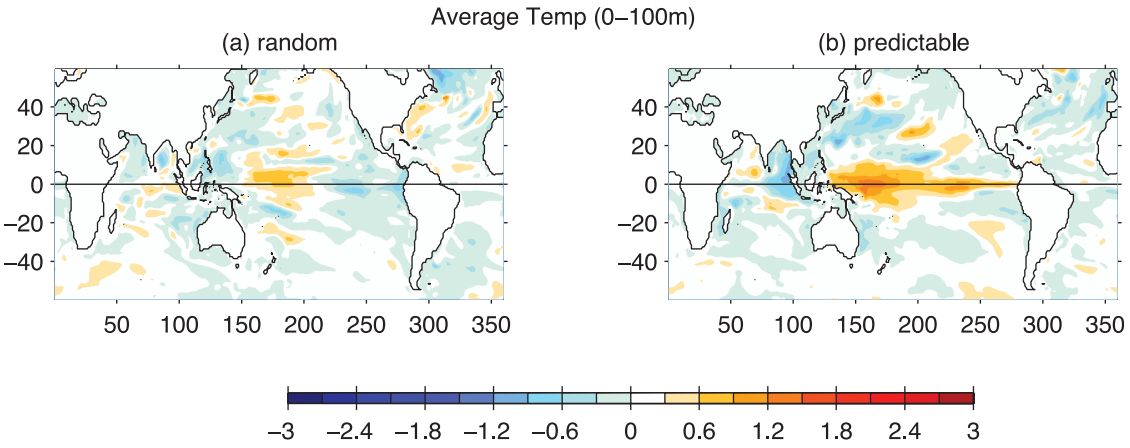

Figure 2. The anomalies of initial average temperature in the upper 100 m of (a) random IODZM composite and (b) predictable IODZM composite. Anomalies are for the initial temperature on 1 January.

and other ocean variables are climatological Jan 1st values. The experiments are run from Jan 1st for one year. It turns out that the experiment with the composite temperature of predictable IODZM produces seven IODZM events, while the experiment with the composite temperature of random IODZM generates two IODZM events (Figures 3a and 3b). Thus, the anomalous ocean heat content pattern shown in Figure 3a is likely the feature that preconditions the climate system of the Indian Ocean to develop into IODZM three seasons hence.

[18] The warming in the western/central equatorial Pacific was identified as a precursor for IODZM in this model by *Song et al.* [2007], and is present in all 5 predictable IODZM events (not shown). However, the cooling in the eastern tropical Indian Ocean is only shared by 2 of the 5 cases (not shown), which suggests that the cooling (~9-month prior to the IODZM) is not a necessary condition. We further examine the relative importance of each individual anomalous ocean heat content pattern (i.e., warming in the western/central equatorial Pacific and cooling in the eastern Indian Ocean) through an additional pair of ensemble predictability experiments. In one experiment, the initial ocean temperature condition consists of composite values of the predictable IODZM category in the tropical

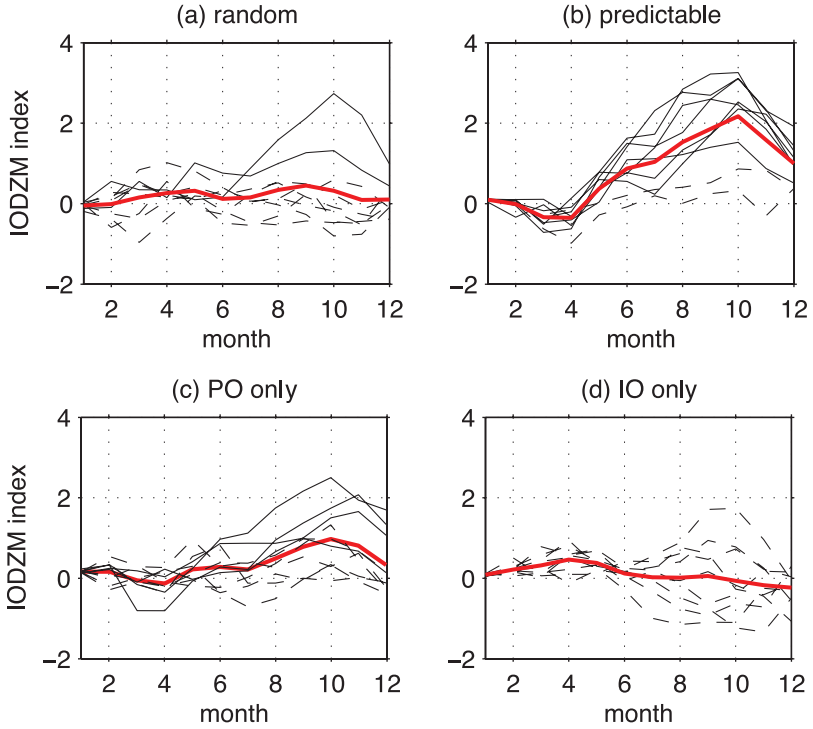

Figure 3. The IODZM index of the two 9-member ensemble experiments initialized from the global composite initial ocean temperature conditions of (a) the random IODZM category and (b) the predictable category; and initialized from the composite initial ocean temperature conditions of the predictable IODZM category (c) only in the tropical Pacific (30°S–30°N), and (d) only for the tropical Indian Ocean (30°S–20°N).

Pacific (30°S–30°N) and climatological Jan 1st values elsewhere. In the second experiment the initial temperature condition consists of composite values of the predictable IODZM category in the tropical Indian Ocean (30°S–20°N) and climatological Jan 1st values elsewhere. The IODZM-I plumes for these experiments are shown in Figures 3c and 3d, indicate that indeed the cooling in the eastern tropical Indian Ocean alone does not lead to any IODZM events, while the warming in the equatorial Pacific leads to 4 IODZM events. This illustrates that in preconditioning the development of IODZM, the upper ocean warming in the western/central equatorial Pacific appears to be an effective feature, while the cooling in the eastern Indian Ocean could be a secondary pattern in the composite due to the small number of predictable IODZM events selected for this study. Note that the number of IODZM events in the experiments initialized by the temperature anomalies of the Pacific Ocean (4 out of 9) is less than that in the experiment initialized by the temperature anomalies of global ocean (7 out of 9) (compare Figures 3b and 3c), yet still more than would be expected from a random sampling. That suggests that, at a three-season lead, temperature anomalies in the Indian Ocean and other part of the world (such as high latitudes, Atlantic) might also play a role, although not a decisive one, in preconditioning the climate system for the development of IODZM events.

5. Summary

[19] In this study we quantify the potential predictability of the SSTAs associated with positive IODZM events within the GFDL coupled climate model framework, under the assumption that model physics is perfect. Instead of assessing the predictability of the overall SSTAs in the Indian Ocean as has been done in previous studies, we focus on three-season lead predictability of positive IODZM years. In this framework, we find that there are two categories of IODZM events, predictable ones and random ones. For predictable IODZM events, prediction skill from the beginning of the IODZM year is possible; and their occurrence largely preconditioned by warm upper ocean heat content anomalies in the western equatorial Pacific. This Pacific warm anomaly pattern resembles that which tends to precede El Niño events, suggesting a connection between predictable IODZM events and El Niño. However, for the random IODZM events, prediction from the beginning of the year is limited. Given the biases inherent in any model, these results should be treated with some degree of caution, and efforts using different model systems should be undertaken to explore the robustness of the results different representation of physical processes. Nonetheless, these results point to new opportunities for further investigation of preconditioning of the IODZM and its seasonal prediction.

[20] **Acknowledgments.** This report was prepared by Qian Song under award NA17RJ2612 from the National Oceanic and Atmospheric Administration, U.S. Department of Commerce. The authors are grateful to the S-I Group at NOAA-GFDL, and Rich Gudgel in particular, for developing and running the GFDL experimental forecast system.

References

Annamalai, H. and R. Murtugudde (2004), Role of the Indian Ocean in regional climate variability, in *Earth Climate: The Ocean-Atmosphere Interaction*, *Geophys. Monogr. Ser.*, vol. 147, edited by C. Wang, S.-P. Xie, and J. A. Carton, pp. 213–246, AGU, Washington, D. C.

Annamalai, H., R. Murtugudde, J. Potemra, S.-P. Xie, P. Liu, and B. Wang (2003), Coupled dynamics over the Indian Ocean: Spring initiation of the Zonal Mode, *Deep Sea Res., Part II*, *50*, 2305–2330.

Baquero-Bernal, A., M. Latif, and S. Legutke (2002), On the dipolelike variability of sea surface temperature in the tropical Indian Ocean, *J. Clim.*, *15*, 1358–1368.

Delworth, T. L., et al. (2006), GFDL's CM2 global coupled climate models. Part 1: Formulation and simulation characteristics, *J. Clim.*, *19*, 643–674.

Fischer, A. S., P. Terray, E. Guilyardi, S. Gualdi, and P. Delecluse (2004), Two independent triggers for the Indian Ocean Dipole/Zonal Mode in a coupled GCM, *J. Clim.*, *18*, 3428–3449.

Gualdi, S., E. Guilyardi, A. Navarra, S. Masina, and P. Delecluse (2003), The interannual variability in the Indian Ocean as simulated by a CGCM, *Clim. Dyn.*, *20*, 567–582.

GFDL Global Atmospheric Model Development Team (GAMDT) (2004), The new GFDL global atmosphere and land model AM2/LM2: Evaluation with prescribed SST simulations, *J. Clim.*, *17*, 4641–4673.

Gnanadesikan, A., et al. (2006), GFDL's CM2 global coupled climate models. Part 2: The baseline ocean simulation, *J. Clim.*, *19*, 675–697.

Griffies, S., M. J. Harrison, R. C. Pacanowski, and A. Rosati (2003), A technical guide to MOM4, *GFDL Ocean Group Tech. Rep. 5*, 295 pp., NOAA Geophys. Fluid Dyn. Lab., Princeton, N. J.

Huang, B., and J. L. Kinter III (2002), Interannual variability in the tropical Indian Ocean, *J. Geophys. Res.*, *107*(C11), 3199, doi:10.1029/2001JC001278.

Iizuka, S., T. Matsuura, and T. Yamagata (2000), The Indian Ocean SST dipole simulated in a coupled general circulation model, *Geophys. Res. Lett.*, *27*, 3369–3372.

Krishnamurthy, V., and B. P. Kirtman (2003), Variability of the Indian Ocean: Relation to monsoon and ENSO, *Q. J. R. Meteorol. Soc.*, *129*, 1623–1646.

Luo, J., S. Masson, S. Behera, and T. Yamagata (2007), Experimental forecasts of the Indian Ocean Dipole using a coupled OAGCM, *J. Clim.*, *20*, 2178–2190.

Murtugudde, R., J. P. McCreary, and A. J. Busalacchi (2000), Oceanic processes associated with anomalous events in the Indian Ocean with relevance to 1997–1998, *J. Geophys. Res.*, *105*, 3295–3306.

Rao, S. A., S. K. Behera, Y. Masumoto, and T. Yamagata (2002), Interannual subsurface variability in the tropical Indian Ocean with a special emphasis on the Indian Ocean dipole, *Deep Sea Res., Part II*, *49*, 1549–1572.

Saji, N. H., B. N. Goswami, P. N. Vinayachandran, and T. Yamagata (1999), A dipole mode in the tropical Indian Ocean, *Nature*, *401*, 360–363.

Saji, N. H., S. P. Xie, and T. Yamagata (2006), Tropical Indian Ocean variability in the IPCC twentieth-century climate simulations, *J. Clim.*, *19*, 4397–4417.

Song, Q., G. A. Vecchi, and A. Rosati (2007), Indian Ocean variability in the GFDL CM2 coupled climate model, *J. Clim.*, *20*, 2895–2916.

Stouffer, R., et al. (2006), GFDL's CM2 global coupled climate models. Part 4: Idealized climate response, *J. Clim.*, *19*, 723–740.

van Oldenborgh, G. J., S. Y. Philip, and M. Collins (2005), El Nino in a changing climate: A multi-model study, *Ocean Sci.*, *1*, 81–95.

Wajsowicz, R. C. (2004), Climate variability over the tropical Indian Ocean sector in the NSIPP seasonal forecast system, *J. Clim.*, *17*, 4783–4804.

Wajsowicz, R. C. (2005a), Forecasting extreme events in the tropical Indian Ocean sector climate, *Dyn. Atmos. Oceans*, *39*, 137–151.

Wajsowicz, R. C. (2005b), Potential predictability of tropical Indian Ocean SST anomalies, *Geophys. Res. Lett.*, *32*, L24702, doi:10.1029/2005GL024169.

Webster, P. J., A. M. Moore, J. P. Loschnigg, and R. R. Leben (1999), Coupled ocean-atmosphere dynamics in the Indian Ocean during 1997–98, *Nature*, *401*, 260–356.

Wittenberg, A. T., A. Rosati, N.-C. Lau, and J. J. Ploshay (2006), GFDL's CM2 global coupled climate models. Part 3: Tropical Pacific climate and ENSO, *J. Clim.*, *19*, 698–722.

Yamagata, T., S. K. Behera, J.-J. Luo, S. Masson, M. R. Jury, and S. A. Rao (2004), Coupled ocean-atmosphere variability in the tropical Indian Ocean, in *Earth Climate: The Ocean-Atmosphere Interaction*, *Geophys. Monogr. Ser.*, vol. 147, edited by C. Wang, S.-P. Xie, and J. A. Carton, pp. 189–211, AGU, Washington, D. C.

A. J. Rosati and G. Vecchi, NOAA Geophysical Fluid Dynamics Laboratory, P.O. Box 308, 201 Forrestal Road, Princeton, NJ 08542, USA. (gabriel.vecchi@noaa.gov)

Q. Song, Program in Atmospheric and Oceanic Sciences, Princeton University, Princeton, NJ 08544, USA.